Letter

# Solving the left-hand cut problem in lattice QCD: $T_{cc}(3875)^+$ from finite volume energy levels

Lu Meng, Vadim Baru, Evgeny Epelbaum, Arseniy A. Filin, and Ashot M. Gasparyan

*Institut für Theoretische Physik II, Ruhr-Universität Bochum, D-44780 Bochum, Germany*

(Received 11 December 2023; accepted 3 April 2024; published 30 April 2024)

We discuss a novel effective-field-theory-based approach for extracting two-body scattering information from finite volume energies, serving as an alternative to Lüscher's method. By explicitly incorporating one-pion exchange, we overcome the challenging left-hand cut problem in Lüscher's method and can handle finite volume energy levels both below and above the left-hand cut. Applied to the lattice data for $DD^*$ scattering at a pion mass of 280 MeV, as an illustrative example, our results reveal the significant impact of the one-pion exchange on $P$-wave and $S$-wave phase shifts. The pole position of the $T_{cc}(3875)^+$ state, extracted from the finite-volume energy levels at this pion mass while taking into account left-hand cut effects, range corrections and partial-wave mixing, is consistent with a near-threshold resonance. This study demonstrates, for the first time, that two-body scattering information can be reliably extracted from lattice spectra including the left-hand cut.

DOI: 10.1103/PhysRevD.109.L071506

*Introduction.* Over the last two decades, numerous exotic hadronic states have been discovered in the heavy quark sector, challenging conventional quark models. Quantum chromodynamics (QCD), with its color confinement, is compatible with a wide range of color-neutral hadrons, such as multiquarks, hadronic molecules, hybrids, glueballs etc., see Refs. [1–8] for the review articles. Yet, the specific configurations that are realized in nature remain enigmatic. Consequently, experimental searches for exotic hadrons and the analysis of data in a manner consistent with unitarity and analyticity, allowing for the appropriate extraction of pole positions, are fundamental for enhancing our understanding of the strong interaction in the Standard Model. Additionally, the pertinent information can be gained from lattice simulations—a first principle approach to solve QCD in a nonperturbative regime, see Refs. [9–14] for recent reviews.

Recently, LHCb observed the first manifestly exotic doubly charmed narrow resonance $T_{cc}(3875)^+$, whose minimal quark content is $cc\bar{u}\bar{d}$ [15,16]. With its mass being just a few hundreds keV below the $D^{*+}D^0$ threshold and the width almost completely dominated by the only available strong decay to $DD\pi$, this state has been extensively analyzed using low-energy effective field theories (EFT) [17–22] and phenomenological models, see, e.g., [7] and references therein.

The $T_{cc}$ has also been recently investigated in lattice QCD [23–25]. In the first two studies, the Lüscher method was employed to determine the $DD^*$ phase shifts (step 1) at pion masses of 280 and 350 MeV, respectively. The extracted infinite-volume phase shifts were then parametrized using the effective-range expansion (ERE) (step 2), leading to the determination of low-energy parameters for $DD^*$ scattering, namely the scattering length and effective range. Furthermore, the pole position determined in Ref. [23] is consistent with the $T_{cc}$ being a virtual state, indicative of its molecular nature [26]. However, the analyses of Refs. [23,24] were questioned in a recent study [27], which highlighted the important role of the one-pion exchange (OPE), which brings a new scale into the problem from a nearby left-hand cut (lhc). The presence of the lhc restricts the ERE, commonly used for analyzing infinite volume phase shifts at step 2, to a very narrow energy range, rendering it unsuitable for accurate pole extractions [27]. Moreover, the validity of the Lüscher formula [28–31], which is the cornerstone for extracting infinite volume amplitudes from finite volume (FV) energy levels at step 1, becomes questionable in the presence of a nearby lhc [32–34].

In this study, we resolve the challenging lhc problem inherent in Lüscher's method, which is fundamental for extracting two-body scattering information from finite volume energy spectra. This achievement is made possible by employing a chiral EFT-based approach, which explicitly incorporates the longest-range interaction from the OPE. We can, therefore, extract infinite volume observables from finite volume energy levels both below and above the lhc. Our method also naturally accounts for range effects and exponentially suppressed corrections related to the OPE [35]. Additionally, the formulation of chiral EFT using the plane wave basis [36] enables us to investigate and understand the impact of partial-wave mixing in a finite volume on the extracted phase shifts.

In parallel to our work, a modified Lüscher formula was proposed to address the lhc problem in Ref. [32]; however, no practical implementations of this approach to lattice data were conducted. To demonstrate our method, we undertake a thorough analysis of lattice energy levels from Ref. [23] to extract, for the first time, the pole of the $T_{cc}$ state while considering all the effects above and quantifying the uncertainties. Our method is general and applicable to the analysis of a wide range of hadronic reactions utilizing lattice energy levels.

*Framework.* In the 1990s, Lüscher established a method that connects the infinite-volume scattering matrix $T(E)$ to the discrete energy levels $E_{\mathrm{FV}}$ of a system in a periodic box [28,29]. The Lüscher formula, also known as Lüscher's quantization conditions (LQCs) can be schematically expressed as [9,13]

$$\det[F^{-1}(E,\mathbf{P},L) - 8\pi i T(E)] = 0, \qquad (1)$$

where $F^{-1}(E,\mathbf{P},L)$ is a known quantity that captures the kinematics of the finite volume. It depends on the box size $L$, the total momentum of the two-body system $\mathbf{P}$ and the total energy $E$. Equation (1) determines a set of lattice energy levels $E_{\mathrm{FV}}$ if the infinite-volume scattering amplitude $T(E)$ is known. However, to obtain observables in the infinite volume, a solution of the inverse problem is required, where $T(E)$ is extracted from $E_{\mathrm{FV}}$. The method is applicable to two-body scattering, including various partial waves and coupled hadron-hadron channels below the lowest three-body threshold. However, while this approach is generally model-independent, it is valid under certain conditions. First, the box size $L$ is required to be significantly larger than the interaction range $R$, in order to justify the neglect of exponentially suppressed corrections $\sim e^{-L/R}$. Yet, for not very large volumes, these exponentially suppressed terms, governed by the longest-range OPE interaction, can be numerically significant [35]. Another complication stems from breaking the rotational symmetry in cubic boxes, which results in energy levels typically receiving contributions from multiple partial waves [29,37]. Partial wave mixing is sometimes disregarded at very low energies due to the threshold suppression of higher partial waves, $T_l \sim E^l$, ensuring a one-to-one correspondence between the phase shifts and the FV energy levels. However, for more general cases where the partial wave mixing effect is significant, this correspondence is lost, and a more complex formalism involving appropriate

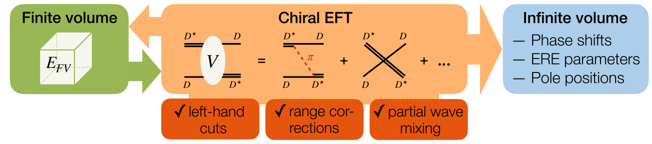


FIG. 1. Schematic illustration of the approach employed in this study. $V$ denotes the effective potential in chiral EFT, involving the OPE and contact interactions; $E_{\mathrm{FV}}$ stands for the finite volume energy levels in lattice simulations, used here as input.

parameterization of the $T$-matrix is required to determine scattering information, see, e.g., [38,39] and references therein. One option for parameterization is the ERE [40], which, however, is only valid in a very narrow energy range limited by the lhc [27]. Finally and most importantly, Lüscher's quantization conditions fail in the presence of the nearby lhc [32,33,41]. Indeed, because the amplitude $T(E)$ is complex below it, while the function $F^{-1}(E,\mathbf{P},L)$ remains real, Eq. (1) can not be applied at least below the lhc.

In this work, we advocate an alternative approach (see also [36]), which allows one to account for all effects discussed above, thereby avoiding the complexity of solving the inverse problem, see Fig. 1 for a schematic illustration. Specifically, we start from the effective Hamiltonian, which incorporates the long-range dynamics due to the OPE and involves contact interactions in relevant partial waves. We then calculate the FV energy spectrum using the plane wave basis with discrete momentum modes and adjust the low-energy constants (LECs), accompanying the contact terms, to achieve the best description of the FV energy levels $E_{\mathrm{FV}}$. The resulting effective Hamiltonian, with all the LECs being fixed to $E_{\mathrm{FV}}$, is then used to calculate the scattering amplitude in the infinite volume.

*Application to $T_{cc}$.* In Ref. [23], the FV energy levels of isospin-0 $DD^*$ scattering were extracted in lattice QCD using the lattice spacing of $a \approx 0.08636$ fm at $m_\pi \approx 280$ MeV, corresponding to the $D$ and $D^*$ meson masses of $M_D = 1927$ MeV and $M_{D^*} = 2049$ MeV, respectively, and two spatial lattice sizes $L = 2.07$ fm and 2.76 fm, as shown in Fig. 2. Following Ref. [23], we consider the nine lowest-lying energy levels in the irreducible representations (irreps) $T_1^+(0)$, $A_1^-(0)$, and $A_2(1)$ of the point groups as input in our calculations. The integer numbers $d$ in the parentheses are related to the total momentum of two particles $\mathbf{P} = \frac{2\pi}{L}\boldsymbol{d}$ with $\boldsymbol{d} \in Z^3$.

Starting from the Lippmann-Schwinger-type integral equations (LSE) in the FV, $\mathbb{T}(E) = \mathbb{V}(E) + \mathbb{V}(E)\mathbb{G}(E)\mathbb{T}(E)$, the FV energy levels are obtained by solving the determinant equation,

$$\det\left[\mathbb{G}^{-1}(E) - \mathbb{V}(E)\right] = 0. \qquad (2)$$

The matrix in the argument of the determinant can be block-diagonalized according to the lattice irreps. Here, the discretized propagator $\mathbb{G}$ is defined as

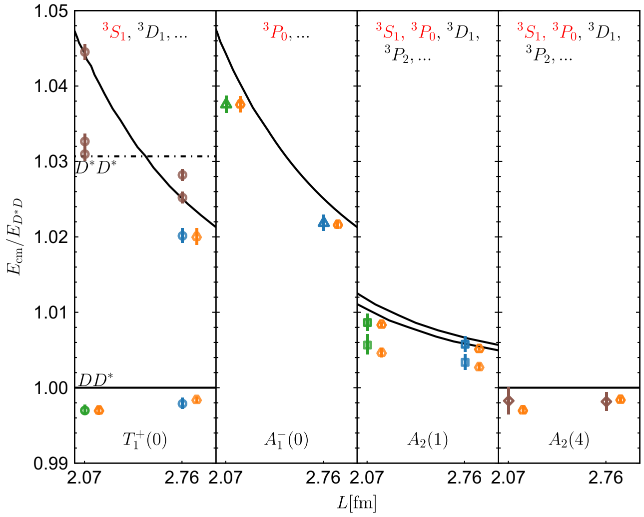


FIG. 2. Fit results for the center-of-mass energy $E_{\rm cm} = \sqrt{E^2 - \mathbf{P}^2}$ of the $DD^*$ system normalized by $E_{DD^*} = M_D + M_{D^*}$, for the heavier charm quark mass and two different volumes from Ref. [23] in various FV irreps. The lattice energy levels are shown by open circles, squares and triangles; the blue and green points in the irreps $T_1^+(0), A_1^-(0)$, and $A_2(1)$ are used as input in this analysis as well as in the scattering analysis of Ref. [23]. The orange symbols, slightly shifted to the right for transparency, represent the results of our full calculation (Fit 2), including pions. For each irrep, we indicate the lowest partial waves, which contribute to it. Our results in the irrep $A_2(4)$ are predictions. The solid and dot-dashed lines correspond to the noninteracting $DD^*$ and $D^*D^*$ energies, respectively.

$$\mathbb{G}_{\boldsymbol{n},\boldsymbol{n}'} = \mathcal{J}\frac{1}{L^3}G(\tilde{p}_{\boldsymbol{n}}, E)\delta_{\boldsymbol{n}',\boldsymbol{n}}, \tag{3}$$

where $\mathcal{J}$ is the Jacobi determinant arising from the transformation between the box and the center-of-mass frames, see Ref. [41] for details, while $\tilde{p}_{\boldsymbol{n}}$ are the discretized momenta. Further, the Green function $G$ reads,

$$G(\tilde{p}, E) = \frac{1}{4\omega_1\omega_2}\left(\frac{1}{E - \omega_1 - \omega_2} - \frac{1}{E + \omega_1 + \omega_2}\right), \tag{4}$$

where $\omega_i = \sqrt{m_i^2 + \tilde{p}^2}$ with $m_1 = M_D$ and $m_2 = M_{D^*}$. To solve Eq. (2) in a finite volume, we use the plane wave basis instead of expanding it in partial waves. This allows us to naturally account for all partial wave mixing effects arising from rotational symmetry breaking in a cubic box [36].

The effective potential $V$ is constructed in chiral EFT up to $\mathcal{O}(Q^2)$, with $Q \sim m_\pi$ being the soft scale of the expansion, and reads,

$$V = V_{\rm OPE}^{(0)} + V_{\rm cont}^{(0)} + V_{\rm cont}^{(2)} + \cdots, \tag{5}$$

where the two-pion exchange contributions at the considered value of $m_\pi$ are assumed to be saturated by the contact terms. Truncating the contact interactions to $\mathcal{O}(Q^2)$, the most relevant contact potentials contributing to the irreps $T_1^+(0), A_1^-(0)$, and $A_2(1)$ read,

$$\begin{aligned} V_{\rm cont}^{(0)+(2)}[^3S_1] &= (C_{^3S_1}^{(0)} + C_{^3S_1}^{(2)}(p^2 + p'^2))(\boldsymbol{\epsilon}\cdot\boldsymbol{\epsilon}'^*) \\ V_{\rm cont}^{(2)}[^3P_0] &= C_{^3P_0}^{(2)}(\boldsymbol{p}'\cdot\boldsymbol{\epsilon}'^*)(\boldsymbol{p}\cdot\boldsymbol{\epsilon}), \end{aligned} \tag{6}$$

where $\boldsymbol{p}$ ($\boldsymbol{p}'$) and $\boldsymbol{\epsilon}$ ($\boldsymbol{\epsilon}'$) denote the center of mass system momentum and polarization of the initial (final) $D^*$ meson, respectively. While the irreps $T_1^+(0)$ and $A_2(1)$ can also receive contributions from the $S$- to $D$-wave short-range interactions as well as from the $^3P_2$ partial waves at $\mathcal{O}(Q^2)$, in what follows, we consider fits with three parameters from Eq. (6) as our main results and use the additional contributions from other partial waves to estimate systematic uncertainties in [41]. The longest-range interaction between the $D$ and $D^*$ mesons is driven by the OPE, which in the static approximation reads,

$$V_{\rm OPE}^{(0)} = -3\frac{M_D M_{D^*} g^2}{f_\pi^2}\frac{(\boldsymbol{k}\cdot\boldsymbol{\epsilon})(\boldsymbol{k}\cdot\boldsymbol{\epsilon}'^*)}{\boldsymbol{k}^2 + \mu^2}, \tag{7}$$

where $\mu^2 = m_\pi^2 - \Delta M^2$, $\Delta M = M_{D^*} - M_D$ and $\boldsymbol{k} = \boldsymbol{p}' + \boldsymbol{p}$. The pion mass dependence of the pion decay constant $f_\pi$ is considered along the lines of Ref. [27,42], which gives $f_\pi = 105.3$ MeV for $m_\pi = 280$ MeV. The value of the coupling constant $g$ is extracted from the fits to its physical value and the lattice data of Ref. [42]. For the given lattice spacing of $a \approx 0.086$ fm and $m_\pi = 280$ MeV, we found $g = 0.517 \pm 0.015$ [41]. When both $p$ and $p'$ are on shell, $p = p' = \frac{\lambda(E^2, M_D^2, M_{D^*}^2)^{1/2}}{2E}$ ($\lambda$ is the Källén function), the OPE and, consequently, the on shell $DD^*$ partial wave amplitudes, exhibit the lhc with the closest to the threshold branch point given by [27]

$$(p_{\rm lhc}^{1\pi})^2 = -\frac{\mu^2}{4} = -(126\ \text{MeV})^2 \Rightarrow \left(\frac{p_{\rm lhc}^{1\pi}}{E_{DD^*}}\right)^2 \approx -0.001, \tag{8}$$

where $E_{DD^*} = M_D + M_{D^*}$. In principle, the OPE may also have the three-body right-hand cut, corresponding to the on shell $DD\pi$ state. However, for $m_\pi = 280$ MeV, it starts at momenta far away from the threshold, $p_{\rm rhc_3}^2 = (552\ \text{MeV})^2$ [27], which makes it irrelevant for the current analysis. It should be noticed that all partial waves are included in Eq. (7), as no partial wave expansion and truncation is made for the OPE in our plane wave expansion method.

The contact interactions in the LSE are supplemented with the exponential regulators of the form $e^{\frac{-(p^n + p'^n)}{\Lambda^n}}$ with $n = 6$. The regularization of the operators with the single pion propagator preserving long-range dynamics is worked out in Ref. [43] and can be implemented by a substitution,

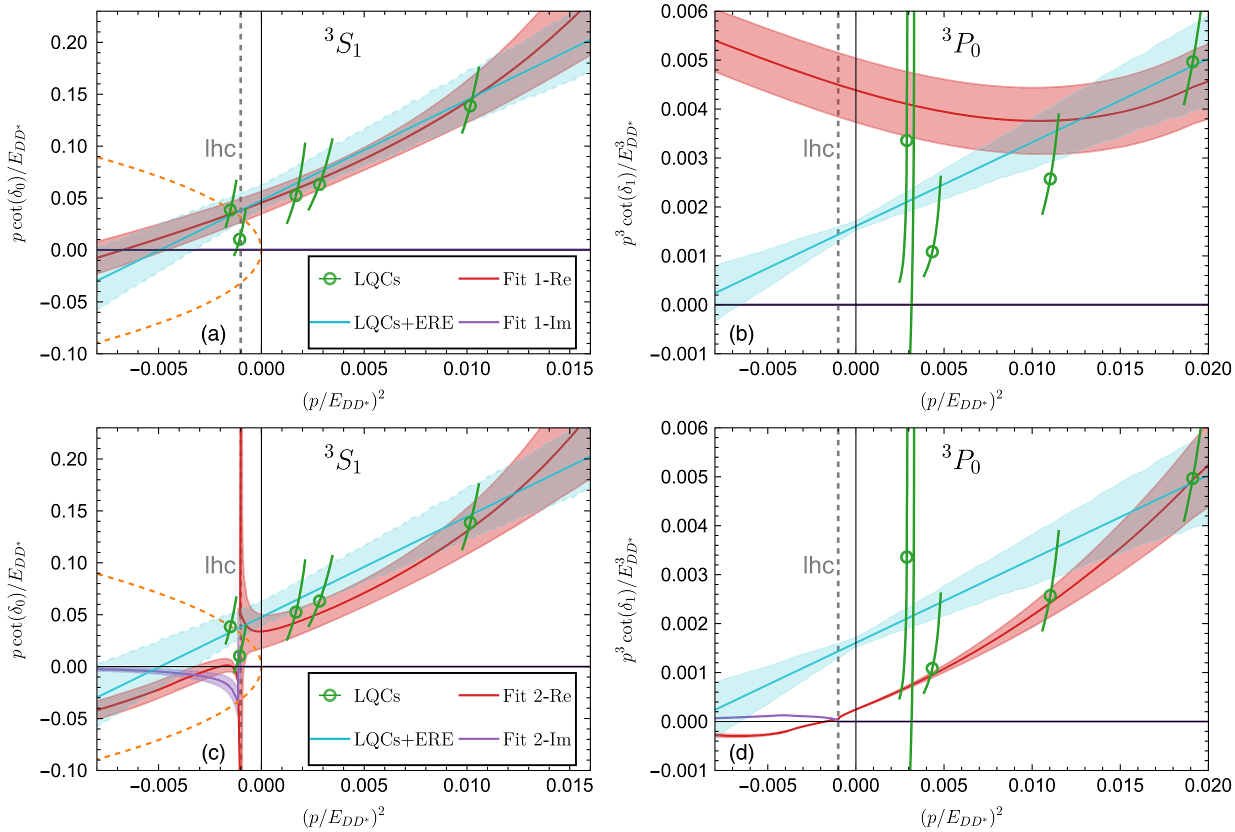


FIG. 3. Phase shifts in the $^3S_1$ (left panel) and $^3P_0$ (right panel) partial waves extracted from the FV energy levels $E_{\mathrm{FV}}$ calculated in lattice QCD. Red bands represent the results of our 3-parameter fits to $E_{\mathrm{FV}}$ *without* the OPE (Fit 1, upper panel) and *with* the OPE (Fit 2, lower panel), including the $1\sigma$ uncertainty. Green dots in the left panel are the phase shifts extracted from $E_{\mathrm{FV}}$ using the single-channel Lüscher quantization conditions in Ref. [23]. Green dots in the right panel are extracted in this study using the same method. Blue bands are the results of the 4-parameter fits of $E_{\mathrm{FV}}$ using the ERE in Ref. [23]. Orange lines in the left panel correspond to $ip = \pm|p|$ from unitarity, normalized to $E_{DD^*}$. The gray vertical dashed line denotes the position of the branch point of the left-hand cut nearest to the threshold.

$$\frac{1}{\boldsymbol{k}^2+\mu^2} \to \frac{1}{\boldsymbol{k}^2+\mu^2} e^{\frac{-(\boldsymbol{k}^2+\mu^2)}{\Lambda^2}}. \tag{9}$$

In what follows, we present the results for the cutoff $\Lambda = 0.9$ GeV and consider the cutoff variation from 0.7 GeV to 1.2 GeV to estimate systematic uncertainties in [41].

To see the impact of the OPE on the results, we perform two calculations: In Fit 1, we start from a pure contact potential without the OPE and adjust the LECs $C^{(0)}_{^3S_1}$, $C^{(2)}_{^3S_1}$, and $C^{(2)}_{^3P_0}$ to obtain the best $\chi^2$ fit to $E_{\mathrm{FV}}$. In Fit 2, we include, in addition to the contact interactions, also the OPE; the corresponding results for the energy levels are shown in Fig. 2. For both fits partial wave mixing is included when calculating $E_{\mathrm{FV}}$ in different lattice irreps. The OPE, however, induces additional mixing between $S$ and $D$ waves due to the long-range tensor interactions. Furthermore, the OPE introduces a new momentum scale related with the branch point of the lhc in Eq. (8), which has several important consequences on the observables: (i) It modifies the analytic structure of the scattering amplitude, making, in particular, the phase shifts complex when analytically continued below the lhc; (ii) It controls the energy dependence of the scattering amplitude in the near-threshold region and (iii) It governs the leading exponentially suppressed corrections $\sim e^{-\mu L}$, neglected in the Lüscher approach.

With the LECs fixed from the best fits to $E_{\mathrm{FV}}$, we are in the position to calculate the infinite volume observables and confront them with the results of the Lüscher analysis of Ref. [23]. In Fig. 3, the results are shown for the phase shifts in the $^3S_1$ and $^3P_0$ partial waves. In the vicinity of the threshold, the phase shifts can be expanded employing the ERE,

$$p^{2l+1}\cot\delta^{(l,J)} = \frac{1}{a^{(l,J)}} + \frac{1}{2} r^{(l,J)} p^2 + \dots. \tag{10}$$

The predictions of Fit 1 for $\delta_{^3S_1}$ (upper left panel) are consistent with the analysis of Ref. [23] using the ERE (10) and also yield very similar values for the ERE parameters and the pole position of the $T_{cc}$ state, as summarized in

TABLE I. Results for the $T_{cc}$ pole position $\delta m_{T_{cc}}$, defined relative to the $DD^*$ threshold, and the $DD^*$ ERE parameters. The results obtained via the Lüscher QCs plus ERE in Ref. [23] are present in the second row. Our results from Fits 1 and 2 are given in the third and forth rows, respectively. The $T_{cc}$ pole position in Fit 2 corresponds to a resonance state with 85% probability within the $1\sigma$ uncertainty. The residual 15% probability corresponds to a scenario with two virtual poles—see the intersection area of the red band with the orange curve in Fig. 3.

| | $a_{^3S_1}$ (fm) | $r_{^3S_1}$ (fm) | $\delta m_{T_{cc}}$ (MeV) | $a_{^3P_0}$ (fm$^3$) | $r_{^3P_0}$ (fm$^{-1}$) | $\chi^2$/d.o.f. |
|---|---|---|---|---|---|---|
| LQCs + ERE fit [23] | $1.04 \pm 0.29$ | $0.96^{+0.18}_{-0.20}$ | $-9.9^{+3.6}_{-7.2}$ | $0.076^{+0.008}_{-0.009}$ | $6.9 \pm 2.1$ | 3.7/5 |
| Fit 1: cont | $1.09 \pm 0.35$ | $0.75 \pm 0.14$ | $-10.6 \pm 4.4$ | $0.028 \pm 0.004$ | $-4.3 \pm 0.05$ | 5.52/6 |
| Fit 2: cont + OPE | $1.46 \pm 0.57$ | $0.096 \pm 0.53$ | $-6.6(\pm 1.5) - i4.0(\pm 3.7)$ | $0.497 \pm 0.007$ | $5.63 \pm 0.19$ | 2.95/6 |

Table I. This is not surprising since both analyses involve two parameters in this partial wave, which can be matched to the scattering length and effective range. On the other hand, the contact fit results for the $\delta_{^3P_0}$ are unable to describe all the data points since the low-energy behavior of the phase shifts can not be captured with a single-parameter fit. To account for the range corrections, the two-parameter fit was introduced in Ref. [23] in line with Eq. (10). This is, however, not needed, since the range corrections in this channel are almost completely driven by the OPE (see our Fit 2 in the lower right panel). The effect of the OPE on $\delta_{^3S_1}$ is also very substantial. The nontrivial interplay of the repulsive OPE and attractive short range interactions results in the appearance of a pole in $p \cot \delta_{^3S_1}$ in the vicinity of the lhc, in line with the results of Ref. [27]. This significantly impacts the validity range of the ERE, the extracted values of the scattering length and effective range, as well as the $T_{cc}$ pole position, which, in our calculation, is highly likely to be a resonance state (see Table I for details). In addition, comparing the phase shifts extracted using the Lüscher approach (green points) with our Fit 2 reveals discrepancies, in particular, for the two lowest-energy datapoints, which are strongly influenced by the lhc. On the other hand, the Lüscher method is consistent with our analysis above the $DD^*$ threshold for both $\delta_{^3S_1}$ and $\delta_{^3P_0}$ phase shifts within errors.

*Summary and outlook.* We discuss a novel approach based on effective field theory to extract information on two-body scattering from finite-volume energies relying on the chiral expansion at low energies. Its main advantage as compared to the Lüscher method consists in the explicit account for the longest-range interaction including the leading left-hand cut, which is crucial for maintaining the appropriate analytic structure of the scattering amplitude near the threshold. Using this method, the finite-volume energy levels can be directly calculated as solutions of the eigenvalue problem both below and above the left-hand cut. It also addresses range effects and the leading exponentially suppressed corrections from the longest-range interaction in a model-independent way. The efficacy of our calculation benefits from using the plane wave basis expansion and the eigenvector continuation; the modern computational technique to fully incorporate the partial-wave mixing effects on lattice and to effectively solve the eigenvalue problem with the small computational cost.

The practical advantages of the approach are demonstrated by making a comprehensive analysis of the lattice energy levels on $DD^*$ scattering from [23] in connection to the doubly charm tetraquark, understanding the properties of which is of fundamental importance in the context of the XYZ exotic states. The long-range interaction from the OPE is demonstrated to significantly influence the understanding of infinite volume observables. Its presence governs the range effects in the $^3P_0$ channel and, contrary to the Lüscher method, allows one to properly calculate amplitudes in the vicinity of the left-hand cut. The systematic corrections related to the truncation of the EFT expansion are shown to be small compared to statistical uncertainties. The extracted pole position of the $T_{cc}^+$ state appears to be most likely a below-threshold resonance shifted to the complex plane due to the OPE. If the uncertainty of the energy levels is substantially reduced, our approach can be used to directly extract the strength of the OPE, represented by the ratio $g/f_\pi$, from lattice data. The incorporation of three-body ($DD\pi$) right-hand cuts is also straightforward and expected to play an important role for analyzing lattice data for lower values of the pion masses (see also [44]).

Our approach is applicable to a wide range of hadronic systems at unphysical pion masses, where finite volume energy levels are already available or will be computed in lattice simulations. For instance, it can enhance our understanding of nucleon-nucleon scattering, where partial wave mixing effects are expected to be important at the physical values of the quark masses and the effects from the lhc are significant [36], and can shed light on hyperon-nucleon and hyperon-hyperon scattering, difficult to obtain otherwise. Consequently, the effect of the lhc is expected to be relevant for probing nuclear structure, neutron stars, $\Sigma$ hypernuclei, $D$-mesic nuclei, etc., but also for understanding exotic hadrons—tetraquarks [23,45], pentaquarks [12], and even six-quark states [34]. These investigations provide important insights into QCD dynamics and its manifestations in the hadron spectrum and reactions.

*Acknowledgments.* The authors are grateful to John Bulava, Jambul Gegelia, and Christoph Hanhart for sharing their insights into the considered topics and to Sasa Prelovsek and Madanagopalan Padmanath for providing us with the covariance matrix and for valuable comments to the manuscript. L. M. is grateful to the helpful discussions with Yan Li and Zi-Yang Lin. This work is supported in part BMBF (Contract No. 05P21PCFP1), by DFG and NSFC through funds provided to the Sino-German CRC 110 "Symmetries and the Emergence of Structure in QCD" (NSFC Grant No. 11621131001, DFG Grant No. TRR110), by the MKW NRW under the Funding Code NW21-024-A and by the EU Horizon 2020 research and innovation programme (STRONG-2020, Grant Agreement No. 824093) and by the European Research Council (ERC) under the EU Horizon 2020 research and innovation programme (ERC AdG NuclearTheory, Grant Agreement No. 885150).

[1] A. Esposito, A. Pilloni, and A. D. Polosa, Multiquark resonances, Phys. Rep. **668**, 1 (2017).
[2] R. F. Lebed, R. E. Mitchell, and E. S. Swanson, Heavy-quark QCD exotica, Prog. Part. Nucl. Phys. **93**, 143 (2017).
[3] F.-K. Guo, C. Hanhart, U.-G. Meißner, Q. Wang, Q. Zhao, and B.-S. Zou, Hadronic molecules, Rev. Mod. Phys. **90**, 015004 (2018).
[4] Y. Yamaguchi, A. Hosaka, S. Takeuchi, and M. Takizawa, Heavy hadronic molecules with pion exchange and quark core couplings: A guide for practitioners, J. Phys. G **47**, 053001 (2020).
[5] N. Brambilla, S. Eidelman, C. Hanhart, A. Nefediev, C.-P. Shen, C. E. Thomas, A. Vairo, and C.-Z. Yuan, The $XYZ$ states: Experimental and theoretical status and perspectives, Phys. Rep. **873**, 1 (2020).
[6] F.-K. Guo, X.-H. Liu, and S. Sakai, Threshold cusps and triangle singularities in hadronic reactions, Prog. Part. Nucl. Phys. **112**, 103757 (2020).
[7] H.-X. Chen, W. Chen, X. Liu, Y.-R. Liu, and S.-L. Zhu, An updated review of the new hadron states, Rep. Prog. Phys. **86**, 026201 (2023).
[8] L. Meng, B. Wang, G.-J. Wang, and S.-L. Zhu, Chiral perturbation theory for heavy hadrons and chiral effective field theory for heavy hadronic molecules, Phys. Rep. **1019**, 1 (2023).
[9] R. A. Briceno, J. J. Dudek, and R. D. Young, Scattering processes and resonances from lattice QCD, Rev. Mod. Phys. **90**, 025001 (2018).
[10] S. Aoki and T. Doi, Lattice QCD and baryon-baryon interactions: HAL QCD method, Front. Phys. **8**, 307 (2020).
[11] M. Mai, M. Döring, and A. Rusetsky, Multi-particle systems on the lattice and chiral extrapolations: A brief review, Eur. Phys. J. Special Topics **230**, 1623 (2021).
[12] P. Bicudo, Tetraquarks and pentaquarks in lattice QCD with light and heavy quarks, Phys. Rep. **1039**, 1 (2023).
[13] J. Bulava *et al.*, Hadron spectroscopy with lattice QCD, in *Snowmass 2021* (2022), arXiv:2203.03230.
[14] S. Prelovsek, Spectroscopy of hadrons with heavy quarks from lattice QCD, arXiv:2310.07341.
[15] R. Aaij *et al.* (LHCb Collaboration), Observation of an exotic narrow doubly charmed tetraquark, Nat. Phys. **18**, 751 (2022).
[16] R. Aaij *et al.* (LHCb Collaboration), Study of the doubly charmed tetraquark $T_{cc}^+$, Nat. Commun. **13**, 3351 (2022).
[17] M. Albaladejo, $T_{cc}^+$ coupled channel analysis and predictions, Phys. Lett. B **829**, 137052 (2022).
[18] L. Meng, G.-J. Wang, B. Wang, and S.-L. Zhu, Probing the long-range structure of the Tcc+ with the strong and electromagnetic decays, Phys. Rev. D **104**, 051502 (2021).
[19] M.-L. Du, V. Baru, X.-K. Dong, A. Filin, F.-K. Guo, C. Hanhart, A. Nefediev, J. Nieves, and Q. Wang, Coupled-channel approach to $T_{cc}^+$ including three-body effects, Phys. Rev. D **105**, 014024 (2022).
[20] E. Braaten, L.-P. He, K. Ingles, and J. Jiang, Triangle singularity in the production of Tcc + (3875) and a soft pion, Phys. Rev. D **106**, 034033 (2022).
[21] B. Wang and L. Meng, Revisiting the $DD^*$ chiral interactions with the local momentum-space regularization up to the third order and the nature of Tcc+, Phys. Rev. D **107**, 094002 (2023).
[22] L. Dai, S. Fleming, R. Hodges, and T. Mehen, Strong decays of Tcc+ at NLO in an effective field theory, Phys. Rev. D **107**, 076001 (2023).
[23] M. Padmanath and S. Prelovsek, Signature of a doubly charm tetraquark pole in $DD^*$ scattering on the lattice, Phys. Rev. Lett. **129**, 032002 (2022).
[24] S. Chen, C. Shi, Y. Chen, M. Gong, Z. Liu, W. Sun, and R. Zhang, $T_{cc}^+(3875)$ relevant $DD^*$ scattering from $N_f = 2$ lattice QCD, Phys. Lett. B **833**, 137391 (2022).
[25] Y. Lyu, S. Aoki, T. Doi, T. Hatsuda, Y. Ikeda, and J. Meng, Doubly charmed tetraquark Tcc+ from lattice QCD near physical point, Phys. Rev. Lett. **131**, 161901 (2023).
[26] I. Matuschek, V. Baru, F.-K. Guo, and C. Hanhart, On the nature of near-threshold bound and virtual states, Eur. Phys. J. A **57**, 101 (2021).
[27] M.-L. Du, A. Filin, V. Baru, X.-K. Dong, E. Epelbaum, F.-K. Guo, C. Hanhart, A. Nefediev, J. Nieves, and Q. Wang, Role of left-hand cut contributions on pole extractions from lattice data: Case study for Tcc(3875)+, Phys. Rev. Lett. **131**, 131903 (2023).
[28] M. Luscher, Volume dependence of the energy spectrum in massive quantum field theories. 2. Scattering states, Commun. Math. Phys. **105**, 153 (1986).
[29] M. Luscher, Two particle states on a torus and their relation to the scattering matrix, Nucl. Phys. **B354**, 531 (1991).
[30] C. H. Kim, C. T. Sachrajda, and S. R. Sharpe, Finite-volume effects for two-hadron states in moving frames, Nucl. Phys. **B727**, 218 (2005).

[31] R. A. Briceno, Two-particle multichannel systems in a finite volume with arbitrary spin, Phys. Rev. D **89**, 074507 (2014).
[32] A. B. a. Raposo and M. T. Hansen, Finite-volume scattering on the left-hand cut, arXiv:2311.18793.
[33] S. M. Dawid, M. H. E. Islam, and R. A. Briceño, Analytic continuation of the relativistic three-particle scattering amplitudes, Phys. Rev. D **108**, 034016 (2023).
[34] J. R. Green, A. D. Hanlon, P. M. Junnarkar, and H. Wittig, Weakly bound $H$ dibaryon from SU(3)-flavor-symmetric QCD, Phys. Rev. Lett. **127**, 242003 (2021).
[35] I. Sato and P. F. Bedaque, Fitting two nucleons inside a box: Exponentially suppressed corrections to the Luscher's formula, Phys. Rev. D **76**, 034502 (2007).
[36] L. Meng and E. Epelbaum, Two-particle scattering from finite-volume quantization conditions using the plane wave basis, J. High Energy Phys. 10 (2021) 051.
[37] L. Leskovec and S. Prelovsek, Scattering phase shifts for two particles of different mass and non-zero total momentum in lattice QCD, Phys. Rev. D **85**, 114507 (2012).
[38] J. J. Dudek, R. G. Edwards, and C. E. Thomas, S and D-wave phase shifts in isospin-2 pi pi scattering from lattice QCD, Phys. Rev. D **86**, 034031 (2012).
[39] A. Woss, C. E. Thomas, J. J. Dudek, R. G. Edwards, and D. J. Wilson, Dynamically-coupled partial-waves in $\rho\pi$ isospin-2 scattering from lattice QCD, J. High Energy Phys. 07 (2018) 043.
[40] C. Morningstar, J. Bulava, B. Singha, R. Brett, J. Fallica, A. Hanlon, and B. Hörz, Estimating the two-particle $K$-matrix for multiple partial waves and decay channels from finite-volume energies, Nucl. Phys. **B924**, 477 (2017).
[41] See Supplemental Material at http://link.aps.org/supplemental/10.1103/PhysRevD.109.L071506 for additional details on our framework, the strategy employed to determine the $D^*D\pi$ coupling constant, fitting procedure and the estimation of systematic uncertainties (2023).
[42] D. Becirevic and F. Sanfilippo, Theoretical estimate of the $D^* \to D\pi$ decay rate, Phys. Lett. B **721**, 94 (2013).
[43] P. Reinert, H. Krebs, and E. Epelbaum, Semilocal momentum-space regularized chiral two-nucleon potentials up to fifth order, Eur. Phys. J. A **54**, 86 (2018).
[44] M. T. Hansen, F. Romero-López, and S. R. Sharpe, Incorporating $DD\pi$ effects and left-hand cuts in lattice QCD studies of the $T_{cc}(3875)^+$, arXiv:2401.06609.
[45] S. Prelovsek and L. Leskovec, Evidence for $X(3872)$ from $DD^*$ scattering on the lattice, Phys. Rev. Lett. **111**, 192001 (2013).